arXiv:2006.08419v4 [stat.ML] 27 Nov 2020

SPHERICAL MOTION DYNAMICS: LEARNING DYNAMICS OF NEURAL NETWORK WITH NORMALIZATION, WEIGHT DECAY, AND SGD

Ruosi Wan[*], **Xiangyu Zhang, Jian Sun**
Megvii Technology
{wanruosi,zhangxiangyu,sunjian}@megvii.com

Zhanxing Zhu[*]
Peking University
{zhanxing.zhu}@pku.edu.cn

ABSTRACT

In this work, we comprehensively reveal the learning dynamics of neural network with normalization, weight decay (WD), and SGD (with momentum), named as Spherical Motion Dynamics (SMD). Most related works study SMD by focusing on "effective learning rate" in "equilibrium" condition, i.e. assuming the convergence of weight norm. However, their discussions on why this equilibrium condition can be reached in SMD is either absent or less convincing. Our work investigates SMD by directly exploring the cause of equilibrium condition. Specifically, 1) we introduce the assumptions that can lead to equilibrium condition in SMD, and prove that weight norm can converge at linear rate with given assumptions; 2) we propose "angular update" as a substitute for effective learning rate to measure the evolving of neural network in SMD, and prove angular update can also converge to its theoretical value at linear rate; 3) we verify our assumptions and theoretical results on various computer vision tasks including ImageNet and MSCOCO with standard settings. Experiment results show our theoretical findings agree well with empirical observations.

1 INTRODUCTION AND BACKGROUND

Normalization techniques (e.g. Batch Normalization (Ioffe & Szegedy, 2015) or its variants) are one of the most commonly adopted techniques for training deep neural networks (DNN). A typical normalization can be formulated as following: consider a single unit in a neural network, the input is $\boldsymbol{X}$, the weight of linear layer is $\boldsymbol{w}$ (bias is included in $\boldsymbol{w}$), then its output is

$$y(\boldsymbol{X};\boldsymbol{w};\gamma;\beta) = g(\frac{\boldsymbol{X}\boldsymbol{w} - \mu(\boldsymbol{X}\boldsymbol{w})}{\sigma(\boldsymbol{w}\boldsymbol{X})}\gamma + \beta), \tag{1}$$

where g is a nonlinear activation function like ReLU or sigmoid, μ, σ are mean and standard deviation computed across specific dimension of $\boldsymbol{X}\boldsymbol{w}$ (like Batch Normalization (Ioffe & Szegedy, 2015), Layer Normalization Ba et al. (2016), Group Normalization (Wu & He, 2018), etc.). β, γ are learnable parameters to remedy for the limited range of normalized feature map. Aside from normalizing feature map, Salimans & Kingma (2016) normalizes weight by l_2 norm instead:

$$y(\boldsymbol{X};\boldsymbol{w};\gamma;\beta) = g(\boldsymbol{X}\frac{\boldsymbol{w}}{||\boldsymbol{w}||_2}\gamma + \beta), \tag{2}$$

where $||\cdot||_2$ denotes l_2 norm of a vector.

[*]Equal Contribution. This work is supported by The National Key Research and Development Program of China (No. 2017YFA0700800) and Beijing Academy of Artificial Intelligence (BAAI). Corresponce to wanruosi@megvii.com.

Characterizing evolving of networks during training. Though formulated in different manners, all normalization techniques mentioned above share an interesting property: the weight $\boldsymbol{w}$ affiliated with a normalized unit is *scale-invariant*: $\forall \alpha \in \mathbb{R}^+, y(\boldsymbol{X}; \alpha \boldsymbol{W}; \gamma, \beta) = y(\boldsymbol{X}; \boldsymbol{w}; \gamma, \beta)$. Due to the scale-invariant property of weight, the Euclidean distance defined in weight space completely fails to measure the evolving of DNN during learning process. As a result, original definition of learning rate η cannot sufficiently represent the update efficiency of normalized DNN.

To deal with such issue, van Laarhoven (2017); Hoffer et al. (2018); Zhang et al. (2019) propose "effective learning rate" as a substitute for learning rate to measure the update efficiency of normalized neural network with stochastic gradient descent (SGD), defined as

$$\eta_{eff} = \frac{\eta}{||\boldsymbol{w}||_2^2}. \tag{3}$$

Joint effects of normalization and weight decay. van Laarhoven (2017) explores the joint effect of normalization and weight decay (WD), and obtains the magnitudes of weight by assuming the convergence of weight, i.e. if $\boldsymbol{w}_t \approx \boldsymbol{w}_{t+1}$, the weight norm can be approximated as $||\boldsymbol{w}_t||_2 \approx O(\sqrt[4]{\eta/\lambda})$, where λ is WD coefficient. Combining with Eq.(3), we have $\eta_{eff} = \sqrt{\eta\lambda}$. A more intuitive demonstration about relationship between normalization and weight decay is presented in Chiley et al. (2019) (see Figure 1): due to the fact that the gradient of scale invariant weight $\partial\mathcal{L}/\partial\boldsymbol{w}$ ($\mathcal{L}$ is the loss function of normalized network without WD part) is always perpendicular to weight $\boldsymbol{w}$, one can infer that gradient component $\partial\mathcal{L}/\partial\boldsymbol{w}$ always tends to increase the weight norm, while the gradient component provided by WD always tends to reduce weight norm. Thus if weight norm remains unchanged, or "equilibrium has been reached"[1], one can obtain

$$\frac{\boldsymbol{w}_t - \boldsymbol{w}_{t+1}}{||\boldsymbol{w}_t||_2} = \sqrt{2\eta\lambda}\frac{\partial\mathcal{L}/\partial\boldsymbol{w}}{\mathbb{E}||\partial\mathcal{L}/\partial\boldsymbol{w}||_2}. \tag{4}$$

Eq.(4) implies the magnitude of update is scale-invariant of gradients, and effective learning rate should be $\sqrt{2\eta\lambda}$. Li & Arora (2020) manages to estimate the magnitude of update in SGDM, their result is presented in limit and accumulation manner: if both $\lim_{T\longrightarrow\infty} R_T = 1/T\sum_{t=0}^{T}||\boldsymbol{w}_t||$ and $\lim_{T\longrightarrow\infty} D_T = 1/T\sum_{t=0}^{T}||\boldsymbol{w}_t - \boldsymbol{w}_{t+1}||$ exist, then we have

$$\lim_{T\longrightarrow\infty}\frac{D_T}{R_T} = \frac{2\eta\lambda}{1+\alpha}. \tag{5}$$

Though not rigorously, one can easily speculate from Eq.(5) the magnitude of update in SGDM cases should be $\sqrt{2\eta\lambda/(1+\alpha)}$ in equilibrium condition. But proof of Eq.(5) requires more strong assumptions: not only convergence of weight norm, but also convergence of update norm $\|\boldsymbol{w}_{t+1} - \boldsymbol{w}_t\|_2$ (both in accumulation manner).

As discussed above, all previous qualitative results about "effective learning rate" (van Laarhoven, 2017; Chiley et al., 2019; Li & Arora, 2020) highly rely on equilibrium condition, but none of them explores why such equilibrium condition can be achieved. Only van Laarhoven (2017) simply interprets the occurrence of equilibrium as a natural result of convergence of optimization, i.e. when optimization is close to be finished, $\boldsymbol{w}_t \approx \boldsymbol{w}_{t+1}$, resulting in equilibrium condition. However, this interpretation has an apparent contradiction: according to Eq.(4) and (5), when equilibrium condition is reached, the magnitude of update is constant, only determined by hyper-parameters, which means optimization process has not converged yet. Li & Arora (2020) also notices the

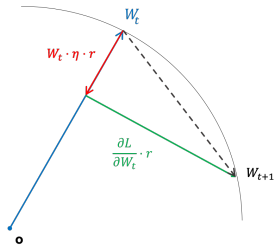


Figure 1: Illustration of optimization behavior with BN and WD. Angular update Δ_t represents the angle between the updated weight $\boldsymbol{W}_t$ and its former value $\boldsymbol{W}_{t+1}$.

[1]"Weight norm remains unchanged" means $||\boldsymbol{w}_t||_2 \approx ||\boldsymbol{w}_{t+1}||_2$, Chiley et al. (2019) calls this condition as "equilibrium", which will also be used in the following context of this paper. Note equilibrium condition is not mathematically rigorous, we only use it for intuitive analysis.

non-convergence of SGD with BN and WD, so they do not discuss reasonableness of assumptions adopted by Eq.(5). In a word, previous results about "effective learning rate" in equilibrium condition can only provide vague insights, they are difficult to be connected with empirical observation.

In this work, we comprehensively reveal the learning dynamics of normalized neural network using stochastic gradient descent without/with momentum (SGD/SGDM) and weight decay, named as **Spherical Motion Dynamics (SMD)**. Our investigation aims to answer the following question,

Why and how equilibrium condition can be reached in Spherical Motion Dynamics?

Specifically, our contributions are

- We introduce the assumptions that can lead to equilibrium condition in SMD, and justify their reasonableness by sufficient experiments. We also prove under given assumptions, equilibrium condition can be reached as weight norm converges to its theoretical value at linear rate in SMD. Our assumptions show the equilibrium condition can occur long before the convergence of the whole optimization;
- We define a novel index, *angular update*, to measure the change of normalized neural network in a single iteration, and derive its theoretical value under equilibrium condition in SMD. We also prove angular update can converge to its theoretical value at linear rate along with convergence of weight norm. Our results imply that the update efficiency of SGD/SGDM on normalized neural network only depends on pre-defined hyper-parameters in both SGD and SGDM case;
- We verify our theorems on different computer vision tasks (including one of most challenging datasets ImageNet (Russakovsky et al., 2015) and MSCOCO (Lin et al., 2014)) with various networks structures and normalization techniques. Experiments show the theoretical value of angular update and weight norm agree well with empirical observation.

2 Related Work

Normalization techniques Batch normalization(BN (Ioffe & Szegedy, 2015)) is proposed to deal with gradient vanishing/explosion, and accelerate the training of DNN. Rapidly, BN has been widely used in almost all kinds of deep learning tasks. Aside from BN, more types of normalization techniques have been proposed to remedy the defects of BN (Ioffe, 2017; Wu & He, 2018; Chiley et al., 2019; Yan et al., 2020) or to achieve better performance (Ba et al., 2016; Ulyanov et al., 2016; Salimans & Kingma, 2016; Shao et al., 2019; Singh & Krishnan, 2020). Though extremely effective, the mechanism of BN still remains as a mystery. Existing works attempt to analyze the function of BN: Ioffe & Szegedy (2015) claims BN can reduce the Internal Covariance Shift (ICS) of DNN; Santurkar et al. (2018) argue that the effectiveness of BN is not related to ICS, but the smoothness of normalized network; Luo et al. (2019) shows BN can be viewed as an implicit regularization technique; Cai et al. (2019) proves that with BN orthogonal least square problem can converge at linear rate; Dukler et al. (2020) proves weight normalization can speed up training in a two-layer ReLU network.

Weight decay Weight decay (WD) is well-known as l_2 regularization, or ridge regression, in statistics. WD is also found to be extreme effective when applied in deep learning tasks. Krizhevsky & Geoffrey (2009) shows WD sometimes can even improve training accuracy not just generalization performance; Zhang et al. (2019) show WD can regularize the input-output Jacobian norm and reduce the effective damping coefficient; Li et al. (2020) discusses the disharmony between WD and weight normalizaiton.

Effective learning rate Due to the scale invariant property caused by normalization, researchers start to study the behavior of effective learning rate. van Laarhoven (2017); Chiley et al. (2019) estimate the magnitude of effective learning rate under equilibrium assumptions in SGD case; Hoffer et al. (2018) quantify effective learning rate without equilibrium assumptions, so their results are much weaker; Arora et al. (2019) proves that without WD, normalized DNN can still converge with fixed/decaying learning rate in GD/SGD cases respectively; Zhang et al. (2019) shows WD can increase effective learning rate; Li & Arora (2020) proves standard multi-stage learning rate

schedule with BN and WD is equivalent to an exponential increasing learning rate schedule without WD. As a proposition, Li & Arora (2020) quantifies the magnitude of effective learning rate in SGDM case. But none of them have ever discussed why equilibrium condition can be reached.

3 PRELIMINARY ON SPHERICAL MOTION DYNAMICS

First of all, we review the property of scale invariant weight, and depict Spherical Motion Dynamics (SMD) in SGD case.

Lemma 1. *If $\boldsymbol{w}$ is scale-invariant with respect to $\mathcal{L}(\boldsymbol{w})$, then for all $k > 0$, we have:*

$$\langle \boldsymbol{w}_t, \frac{\partial \mathcal{L}}{\partial \boldsymbol{w}}\Big|_{\boldsymbol{w}=\boldsymbol{w}_t} \rangle = 0 \tag{6}$$

$$\frac{\partial \mathcal{L}}{\partial \boldsymbol{w}}\Big|_{\boldsymbol{w}=k\boldsymbol{w}_t} = \frac{1}{k} \cdot \frac{\partial \mathcal{L}}{\partial \boldsymbol{w}}\Big|_{\boldsymbol{w}=\boldsymbol{w}_t}. \tag{7}$$

Proof can be seen in Appendix A.1. Lemma 1 is also discussed in Hoffer et al. (2018); van Laarhoven (2017); Li & Arora (2020). Eq.(7) implies gradient norm is influenced by weight norm, but weight norm does not affect the output of DNN, thus we define **unit gradient** to eliminate the effect of weight norm.

Definition 1 (Unit Gradient). *If $\boldsymbol{w}_t \neq \boldsymbol{0}$, $\tilde{\boldsymbol{w}} = \boldsymbol{w}/||\boldsymbol{w}||_2$, the unit gradient of $\partial\mathcal{L}/\partial\boldsymbol{w}|_{\boldsymbol{w}=\boldsymbol{w}_t}$ is $\partial\mathcal{L}/\partial\boldsymbol{w}|_{\boldsymbol{w}=\tilde{\boldsymbol{w}}_t}$.*

According to Eq.(7), we have

$$\frac{\partial \mathcal{L}}{\partial \boldsymbol{w}}\Big|_{\boldsymbol{w}=\boldsymbol{w}_t} = \frac{1}{||\boldsymbol{w}_t||} \cdot \frac{\partial \mathcal{L}}{\partial \boldsymbol{w}}\Big|_{\boldsymbol{w}=\tilde{\boldsymbol{w}}_t}. \tag{8}$$

A typical SGD update rule without WD is

$$\boldsymbol{w}_{t+1} = \boldsymbol{w}_t - \eta \frac{\partial \mathcal{L}}{\partial \boldsymbol{w}}\Big|_{\boldsymbol{w}=\boldsymbol{w}_t}, \tag{9}$$

if $||\boldsymbol{w}_t||_2 \approx ||\boldsymbol{w}_{t+1}||_2$, one can obtain

$$\tilde{\boldsymbol{w}}_{t+1} = \tilde{\boldsymbol{w}}_t - \frac{\eta}{||\boldsymbol{w}_t||_2^2} \frac{\partial \mathcal{L}}{\partial \boldsymbol{w}}\Big|_{\boldsymbol{w}=\tilde{\boldsymbol{w}}_t} = \tilde{\boldsymbol{w}}_t - \eta_{eff} \cdot \frac{\partial \mathcal{L}}{\partial \boldsymbol{w}}\Big|_{\boldsymbol{w}=\tilde{\boldsymbol{w}}_t}. \tag{10}$$

Eq.(10) shows effective learning rate can be viewed as learning rate of SGD on unit sphere $\mathcal{S}^{p-1}$ (Hoffer et al., 2018). But effective learning rate still cannot properly represent the magnitude of update, since unit gradient norm is unknown. Therefore we propose the **angular update** defined below.

Definition 2 (Angular Update). *Assuming $\boldsymbol{w}_t$ is a scale-invariant weight from a neural network at iteration t, then the **angular update** Δ_t is defined as*

$$\Delta_t = \measuredangle(\boldsymbol{w}_t, \boldsymbol{w}_{t+1}) = arccos\left(\frac{\langle \boldsymbol{w}_t, \boldsymbol{w}_{t+1} \rangle}{||\boldsymbol{w}_t|| \cdot ||\boldsymbol{w}_{t+1}||}\right), \tag{11}$$

where $\measuredangle(\cdot,\cdot)$ denotes the angle between two vectors, $\langle \cdot,\cdot \rangle$ denotes the inner product.

According to Eq.(6), $\partial\mathcal{L}/\partial\boldsymbol{w}$ is perpendicular to weight $\boldsymbol{w}$. Therefore, if learning rate η is small enough, one can derive

$$\Delta_t \approx \tan(\Delta_t) = \frac{\eta}{||\boldsymbol{w}_t||} \cdot ||\frac{\partial \mathcal{L}}{\partial \boldsymbol{w}}\Big|_{\boldsymbol{w}=\boldsymbol{w}_t}||_2. \tag{12}$$

Another deduction from Eq.(6) is that weight norm always increases because

$$||\boldsymbol{w}_{t+1}||_2^2 = ||\boldsymbol{w}_t||_2^2 + (\eta||\frac{\partial \mathcal{L}}{\partial \boldsymbol{w}}\Big|_{\boldsymbol{w}=\boldsymbol{w}_t}||_2)^2 > ||\boldsymbol{w}_t||_2^2. \tag{13}$$

From Eq.(7) we can infer that increasing weight norm can lead to smaller gradient norm if unit gradient norm is unchanged. Zhang et al. (2019) states the potential risk that GD/SGD without WD but BN will converge to a stationary point not by reducing loss but by reducing effective learning rate

due to increasing weight norm. Arora et al. (2019) proves that full gradient descent can avoid such problem and converge to a stationary point defined in $\mathcal{S}^{p-1}$, but their results still require sophisticated learning rate decay schedule in SGD case. Besides, practical implementation suggests training DNN without WD always suffers from poor generalization.

Now considering the update rule of SGD with WD:

$$\boldsymbol{w}_{t+1} = \boldsymbol{w}_t - \eta(\frac{\partial \mathcal{L}}{\partial \boldsymbol{w}}\Big|_{\boldsymbol{w}=\boldsymbol{w}_t} + \lambda \boldsymbol{w}_t). \tag{14}$$

We can easily derive the update of weight norm by

$$||\boldsymbol{w}_{t+1}||_2 \approx ||\boldsymbol{w}_t||_2 - \lambda\eta||\boldsymbol{w}_t||_2 + \frac{\eta^2}{2||\boldsymbol{w}_t||_2^3} \cdot ||\frac{\partial \mathcal{L}}{\partial \boldsymbol{w}}\Big|_{\boldsymbol{w}=\tilde{\boldsymbol{w}}_t}||_2^2. \tag{15}$$

Eq.(15) implies WD can provide direction to reduce weight norm, hence Chiley et al. (2019); Zhang et al. (2019) point out the possibility that weight norm can be steady, but do not explain this clearly. Here we demonstrate the mechanism deeper (see Figure 1): if unit gradient norm remains unchanged, note "centripetal force" ($-\lambda\eta||\boldsymbol{w}_t||_2$) is proportional to weight norm, while "centrifugal force" ($\frac{\eta^2}{2||\boldsymbol{w}_t||_2^3} \cdot ||\frac{\partial \mathcal{L}}{\partial \boldsymbol{w}}\Big|_{\boldsymbol{w}=\tilde{\boldsymbol{w}}_t}||_2^2$) is inversely proportional cubic weight norm. As a result, the dynamics of weight norm is like a spherical motion in physics: overly large weight norm makes centripetal force larger than centrifugal force, leading to decreasing weight norm; while too small weight norm makes centripetal force smaller than centrifugal force, resulting in the increase of weight norm. Intuitively, equilibrium condition tends to be reached if the number of iterations is sufficiently large.

Notice that the core assumption mentioned above is "unit gradient norm is unchanged". In fact this assumption can solve the contradiction we present in Section 1: the convergence of weight norm is not equivalent to convergence of weight, steady unit gradient norm can also make weight norm converge, steady unit gradient norm does not rely on the fact that optimization has reached an optimum solution. In next section, We formulate this assumption in a reasonable manner, and rigorously prove the existence of equilibrium condition in SGD case. Discussion about SGD cannot be easily extended to SGDM case, because momentum is not always perpendicular to weight as unit gradient. But we can still prove the convergence of weight norm in SGDM case under modified assumptions.

4 Main Results

First of all, we prove the existence of equilibrium condition in SGD case and provide the convergence rate of weight norm.

Theorem 1. ***(Equilibrium condition in SGD)*** *Assume the loss function is $\mathcal{L}(\boldsymbol{X}; \boldsymbol{w})$ with scale-invariant weight $\boldsymbol{w}$, denote $\boldsymbol{g}_t = \frac{\partial \mathcal{L}}{\partial \boldsymbol{w}}\big|_{\boldsymbol{X}_t, \boldsymbol{w}_t}$, $\tilde{\boldsymbol{g}}_t = \boldsymbol{g}_t \cdot ||\boldsymbol{w}_t||_2$. Considering the update rule of SGD with weight decay,*

$$\boldsymbol{w}_{t+1} = \boldsymbol{w}_t - \eta \cdot (\boldsymbol{g}_t + \lambda \boldsymbol{w}_t) \tag{16}$$

where $\lambda, \eta \in (0, 1)$. If the following assumptions hold: 1) $\lambda\eta << 1$; 2) $\exists L, V, \in \mathbb{R}^+$, $\mathbb{E}[||\tilde{\boldsymbol{g}}_t||_2^2|\boldsymbol{w}_t] = L$, $\mathbb{E}[(||\tilde{\boldsymbol{g}}_t||_2^2 - L)^2|\boldsymbol{w}_t] \leq V$; 3) $\exists l \in \mathbb{R}^+$, $||\tilde{\boldsymbol{g}}_t||_2^2 > l$, $l > 2[\frac{2\lambda\eta}{1-2\lambda\eta}]^2 L$. Then $\exists B > 0$, $w^* = \sqrt[4]{L\eta/(2\lambda)}$, we have

$$\mathbb{E}[||\boldsymbol{w}_T||_2^2 - (w^*)^2]^2 \leq (1 - 4\lambda\eta)^T B + \frac{V\eta^2}{l}. \tag{17}$$

Remark 1. *The theoretical value of weight norm w^* in Theorem 1 is consistent with the derivation of weight norm in equilibrium in van Laarhoven (2017), though van Laarhoven (2017) assumes the equilibrium condition has been reached in advance, hence it cannot provide the convergence rate and magnitude of variance.*

Proof of Theorem 1 can be seen in Appendix A.2. It shows the square of weight norm can linearly converge to its theoretical value in equilibrium, and its variance is bounded by the variance of the square of unit gradient norm multiplying the square of learning rate. Now we discuss the reasonableness of assumptions in Theorem 1. Assumption 1 is consistent with commonly used settings;

assumptions 2 and 3 imply the expectation of the square of unit gradient norm remains unchanged within several iterations, and its lower bound cannot be far from its expectation. We need to clarify assumption 2 further: we do not require the expectation of the unit gradient norm must be constant across the whole training process, but only remains unchanged locally. On one hand, small learning rate can guarantee the expectation of unit gradient norm square changes slowly; on the other hand, when its expectation changes, it means that the weight norm square will change to its new theoretical value as Theorem 1 describes. Experiment result in Figure 2 strongly justifies our analysis. We also conduct extensive experiments to verify our claim further, please refer Appendix B.1.

Now we extend Theorem 1 to SGDM case. SGDM is more complex than SGD since momentum is not always perpendicular to the weight, therefore we need to modify assumptions.

Theorem 2. ***(Equilibrium condition in SGDM)*** *Considering the update rule of SGDM (heavy ball method (Polyak, 1964)):*

$$\boldsymbol{v}_t = \alpha \boldsymbol{v}_{t-1} + \boldsymbol{g}_t + \lambda \boldsymbol{w}_t \tag{18}$$

$$\boldsymbol{w}_{t+1} = \boldsymbol{w}_t - \eta \boldsymbol{v}_t \tag{19}$$

where $\lambda, \eta, \alpha \in (0, 1)$. *If following assumptions hold: 4)* $\lambda\eta << 1$, $\lambda\eta < (1 - \sqrt{\alpha})^2$*; 5) Define* $h_t = ||\boldsymbol{g}_t||_2^2 + 2\alpha\langle \boldsymbol{v}_{t-1}, \boldsymbol{g}_t\rangle$, $\tilde{h}_t = h_t \cdot ||\boldsymbol{w}_t||_2^2$. $\exists L, V, \in \mathbb{R}^+$, $\mathbb{E}[\tilde{h}_t|\boldsymbol{w}_t] = L$, $\mathbb{E}[(\tilde{h}_t - L)^2|\boldsymbol{w}_t] \leq V$*; 6)*$\exists l \in \mathbb{R}^+$, $h_t > l$, $l > 2[\frac{6\lambda\eta}{(1-\alpha)^3(1+\alpha)-8\lambda\eta(1-\alpha)}]^2 L$. *then* $\exists B > 0$, $w^* = \sqrt[4]{L\eta/(\lambda(1-\alpha)(2-\lambda\eta/(1+\alpha)))}$*, we have*

$$\mathbb{E}[||\boldsymbol{w}_T||_2^2 - (w^*)^2]^2 \leq 3B \cdot (1 - \frac{4\lambda\eta}{1-\alpha})^T + \frac{3V\eta^2(1+4\alpha^2+\alpha^4)}{l(1-\alpha)^4}, \tag{20}$$

Proof can be seen in Appendix. Like assumption 1, assumption 4 is also satisfied for commonly used hyper-parameter settings. Besides, $\lambda\eta < (1 - \sqrt{\alpha})^2$ is also mentioned in Li & Arora (2020) for other purpose; Assumption 5 shows not unit gradient gradient norm $||\tilde{\boldsymbol{g}}_t||_2^2$ but an adjusted value $\tilde{h}_t$ dominates the expectation and variance of the weight norm square. We empirically find the expectation of $\langle \boldsymbol{v}_{t-1}, g_t\rangle$ is very close to 0, therefore the behavior of $\tilde{h}_t$ is similar to that of $||\tilde{\boldsymbol{g}}_t||_2^2$ (see (d) in Figure 2), making the weight norm square linearly converge in SGDM case. We leave theoretical analysis on $\tilde{h}_t$ as future work. As for assumption 6, commonly used settings ($\eta\lambda << 1$) can make $2[\frac{6\lambda\eta}{(1-\alpha)^3(1+\alpha)-8\lambda\eta(1-\alpha)}]^2$ as an very small lower bound for l/L. The experiments on justification of assumptions 4,5,6 can be seen in Figure 2 and appendix B.1. Comparing with Eq.(17) and Eq.(20), it implies that with same η, λ, SGDM can reach equilibrium condition much faster than SGD, but may have a larger variance, our experiments also verify that(see (b), (e) in Figure 2).

Since the convergence of weight norm in SMD has been proven, we can drive the theoretical value of angular update Δ_t and its rate of convergence.

Theorem 3. ***(The convergence of angular update)*** *In SGD case, if* $||\tilde{\boldsymbol{g}}_t^2||_2$ *remains unchanged* ($V = 0$)*,* $\exists C > 0$ *we have*

$$|\Delta_t - \sqrt{2\lambda\eta}| < C(1 - \eta\lambda)^t \tag{21}$$

In SGDM case, if $\tilde{h}_t$ *remains unchanged* ($V = 0$)*,* $\exists C > 0$ *we have*

$$|\Delta_t - \sqrt{\frac{2\lambda\eta}{1+\alpha}}| < C(1 - \frac{\eta\lambda}{1-\alpha})^t \tag{22}$$

Remark 2. *Theoretical value of angular update in Theorem 3 is consistent with Chiley et al. (2019); Li & Arora (2020) respectively. Note that we only present the convergence rate of angular update in ideal cases, i.e.* $||\tilde{\boldsymbol{g}}_t^2||_2$ *or* $\tilde{h}_t$ *remain unchanged across the whole training process, because though Eq.(17) and (20) imply that the variance of weight norm square is very small* ($O(\eta^2)$) *with small learning rate, this bound is not tight enough to properly estimate the variance of angular update. Numerical experiments(see Figure 4, 5 in appendix B.1) show the variance of weight norm and angular update can be extremely small, we leave this theoretical gap as future work.*

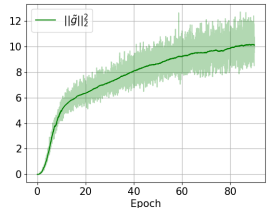
5 EXPERIMENTS

In this section, we show that our theorems can agree well with empirical observations on ImageNet (Russakovsky et al., 2015) and MSCOCO (Lin et al., 2014). We conduct experiments in two

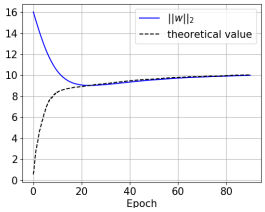
cases. In the first case we train neural network with fixed learning rate to verify our theorems in SGD and SGDM, respectively; in the second case we investigate SMD with more commonly used settings, multi-stage learning rate schedule.

5.1 FIXED LEARNING RATE

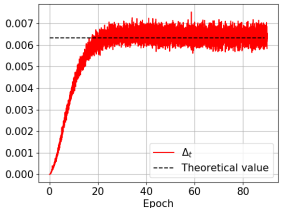
With fixed learning rate, we train Resnet50 (He et al., 2016) with SGD/SGDM on ImageNet. Learning rate is fixed as $\eta = 0.2$; WD factor is $\lambda = 10^{-4}$; with SGDM, the momentum factor is $\alpha = 0.9$. Figure 2 presents the unit gradient norm square, weight norm, and angular update of the weights from LAYER.2.0.CONV2 of Resnet50 in SGD and SGDM cases, respectively. It can be inferred from Figure 2 the behavior of $||\tilde{\boldsymbol{g}}_t||_2^2$, $\tilde{h}_t$ and hyper-parameter settings satisfy our assumptions in Theorem 1 and 2, therefore theoretical value of weight norm and angular update agree with empirical value very well. We also can observe SGDM can achieve equilibrium more quickly than SGD. According to Eq.(17),(20), the underlying reason might be with same learning rate η and WD factor λ, convergence rate of SGDM $(1 - \frac{\lambda\eta}{1-\alpha})$ is smaller than that of SGD $(1 - \lambda\eta)$.



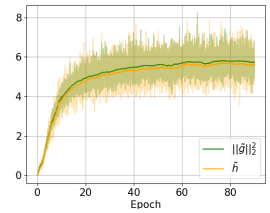
(a) Unit gradient norm in SGD



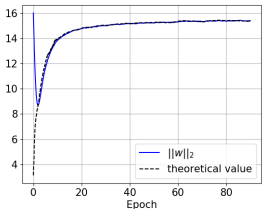
(b) Weight norm in SGD



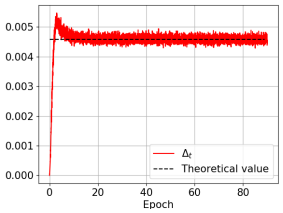
(c) Angular update in SGD



(d) Unit gradient norm square and $\tilde{h}$ in SGDM



(e) Weight norm in SGDM

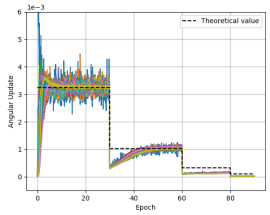


(f) Angular update in SGDM

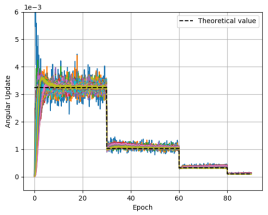
Figure 2: Performance of *layer.2.0.conv2* from Resnet50 in SGD and SGDM, respectively. In (a), (d), semitransparent line represents the raw value of $||\tilde{\boldsymbol{g}}_t||_2^2$ or $\tilde{h}_t$, while solid line represents the averaged value within consecutive 200 iterations to estimate the expectation of $||\tilde{\boldsymbol{g}}_t||_2^2$ or $\tilde{h}_t$; In (b), (e), blue solid lines shows the raw value of weight norm $||\boldsymbol{w}_t||_2$, while dashed line represent the theoretical value of weight norm computed in Theorem 1, 2 respectively. The expectations of $||\tilde{\boldsymbol{g}}||_2^2$ and $\tilde{h}$ are estimated as (a) and (d) respectively; In (c), (f), red lines represent raw value of angular update during training, dashed lines represent the theoretical value of angular update computed by $\sqrt{2\lambda\eta}$ and $\sqrt{2\lambda\eta/(1+\alpha)}$ respectively.

5.2 MULTI-STAGE LEARNING RATE SCHEDULE

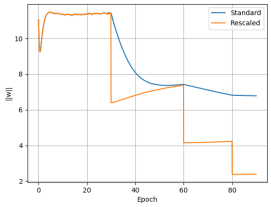
Now we turn to study the behavior of angular update with SGDM and multi-stage leanring rate schedule on Imagenet (Russakovsky et al., 2015) and MSCOCO (Lin et al., 2014). In ImageNet classification task, we still adopt Resnet50 as baseline for it is a widely recognized network structure.The training settings rigorously follow Goyal et al. (2017): learning rate is initialized as 0.1, and divided by 10 at 30, 60, 80-th epoch; the WD factor is 10^{-4}; the momentum factor is 0.9. In MSCOCO experiment, we conduct experiments on Mask-RCNN (He et al., 2017) benchmark using a Feature Pyramid Network (FPN) (Lin et al., 2017), ResNet50 backbone and SyncBN (Peng et al., 2018) following the 4x setting in He et al. (2019): total number of iteration is $360,000$, learning rate is initialized as 0.02, and divided by 10 at iteration $300,000$, $340,000$; WD coefficient is 10^{-4}.



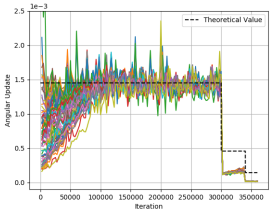
(a) Angular update in Imagenet



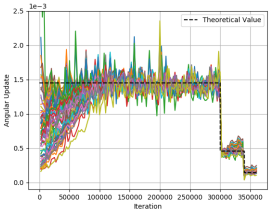
(b) Angular update in Imagenet (rescaled)



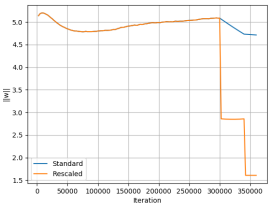
(c) Weight norm in Imagenet



(d) Angular update in MSCOCO



(e) Angular update in MSCOCO (rescaled)



(f) Weight norm in MSCOCO

Figure 3: In (a),(b),(d),(e), solid lines with different colors represent raw value of angular update of weights from all convolutional layer in the model; In (a), (d), training setting rigorously follows Goyal et al. (2017); He et al. (2019) respectively; In (b), (e), weight norm is dividied by $\sqrt[4]{10}$ as long as learning rate is divided by 10; In (c), (f), weight norm is computed on *layer.1.0.conv2* in Resnet50 backbone. Blue line represent original settings, orange line represent rescaled settings.

There appears to be some mismatch between theorems and empirical observations in (a), (b) of Figure 3: angular update in the last two stages is smaller than its theoretical value. This phenomenon can be well interpreted by our theory: according to Theorem 1, 2, when equilibrium condition is reached, theoretical value of weight norm satisfies $||\boldsymbol{w}_t||_2 \propto \sqrt[4]{\frac{\eta}{\lambda}}$, therefore when learning rate is divided by k, equilibrium condition is broken, theoretical value of weight norm in new equilibrium condition should get $\sqrt[4]{1/k}$ smaller. But new equilibrium condition cannot be reached immediately (see (c), (f) in Figure 3), following corollary gives the least number of iterations to reach the new equilibrium condition.

Corollary 3.1. *In SGD case with learning rate η, WD coefficient λ, if learning rate is divided by k, and unit gradient norm remains unchanged, then at least $\lceil[\log(k)]/(4\lambda\eta)\rceil$ iterations are required to reach the new equilibrium condition; In SGDM case with momentum coefficient α, then at least $\lceil[\log(k)(1-\alpha)]/(4\lambda\eta)\rceil$ iterations are required to reach the new equilibrium condition.*

Corollary 3.1 also implies SGD/SGDM with smaller learning rate requires more iterations to reach new equilibrium condition. Hence, in second learning rate stage in Imagenet experiments, angular update can reach its new theoretical value within 15 epochs, but during last two learning rate stages of Imagenet/MSCOCO experiments, SGDM cannot completely reach new equilibrium by the end of training procedure. As a result, we observe empirical value of angular update seems smaller than its theoretical value. Based on our theorem, we can bridge the gap by skipping the intermediate process from old equilibrium to new one. Specifically, when learning rate is divided by k, norm of scale-invariant weight is also divided by $\sqrt[4]{k}$, SGDM can reach in new equilibrium immediately. Experiments((b),(e) in Figure 3) show this simple strategy can make angular update always approximately equal to its theoretical value across the whole training process though learning rate changes.

6 Conclusion

In this paper, we comprehensively reveal the learning dynamics of DNN with normalization, WD, and SGD/SGDM, named as Spherical Motion Dynamics (SMD). Different from most related works (van Laarhoven, 2017; Hoffer et al., 2018; Chiley et al., 2019; Li & Arora, 2020), we directly explore the cause of equilibrium. Specifically, we introduce the assumptions that can lead to equilibrium condition, and show these assumptions are easily satisfied by practical implementation of DNN; Under given assumptions, we prove equilibrium condition can be reached at linear rate, far

before optimization has converged. Most importantly, we show our theorem is widely valid, they can be verified on one of most challenging computer vision tasks, beyond synthetic datasets. We believe our theorems on SMD can bridge the gap between current theoretical progress and practical usage on deep learning techniques.

REFERENCES

Sanjeev Arora, Zhiyuan Li, and Kaifeng Lyu. Theoretical analysis of auto rate-tuning by batch normalization. In *International Conference on Learning Representations*, 2019. URL https://openreview.net/forum?id=rkxQ-nA9FX.

Jimmy Lei Ba, Jamie Ryan Kiros, and Geoffrey E Hinton. Layer normalization. *arXiv preprint arXiv:1607.06450*, 2016.

Yongqiang Cai, Qianxiao Li, and Zuowei Shen. A quantitative analysis of the effect of batch normalization on gradient descent. In Kamalika Chaudhuri and Ruslan Salakhutdinov (eds.), *Proceedings of the 36th International Conference on Machine Learning*, volume 97 of *Proceedings of Machine Learning Research*, Long Beach, California, USA, 09–15 Jun 2019. PMLR. URL http://proceedings.mlr.press/v97/cai19a.html.

Vitaliy Chiley, Ilya Sharapov, Atli Kosson, Urs Koster, Ryan Reece, Sofia Samaniego de la Fuente, Vishal Subbiah, and Michael James. Online normalization for training neural networks. In *Advances in Neural Information Processing Systems 32*, pp. 8433–8443. Curran Associates, Inc., 2019.

Yonatan Dukler, Quanquan Gu, and Guido Montúfar. Optimization theory for relu neural networks trained with normalization layers. In *International conference on machine learning*, 2020.

Priya Goyal, Piotr Dollár, Ross Girshick, Pieter Noordhuis, Lukasz Wesolowski, Aapo Kyrola, Andrew Tulloch, Yangqing Jia, and Kaiming He. Accurate, large minibatch sgd: Training imagenet in 1 hour. *arXiv preprint arXiv:1706.02677*, 2017.

Kaiming He, Xiangyu Zhang, Shaoqing Ren, and Jian Sun. Deep residual learning for image recognition. In *Proceedings of the IEEE conference on computer vision and pattern recognition*, pp. 770–778, 2016.

Kaiming He, Georgia Gkioxari, Piotr Dollár, and Ross Girshick. Mask r-cnn. In *Proceedings of the IEEE international conference on computer vision*, pp. 2961–2969, 2017.

Kaiming He, Ross Girshick, and Piotr Dollar. Rethinking imagenet pre-training. In *Proceedings of the IEEE/CVF International Conference on Computer Vision (ICCV)*, October 2019.

Elad Hoffer, Ron Banner, Itay Golan, and Daniel Soudry. Norm matters: efficient and accurate normalization schemes in deep networks. In S. Bengio, H. Wallach, H. Larochelle, K. Grauman, N. Cesa-Bianchi, and R. Garnett (eds.), *Advances in Neural Information Processing Systems 31*, pp. 2160–2170. Curran Associates, Inc., 2018.

Sergey Ioffe. Batch renormalization: Towards reducing minibatch dependence in batch-normalized models. In *Advances in neural information processing systems*, pp. 1945–1953, 2017.

Sergey Ioffe and Christian Szegedy. Batch normalization: Accelerating deep network training by reducing internal covariate shift. In *ICML*, pp. 448–456, 2015.

Alex Krizhevsky and Hinton Geoffrey. Learning multiple layers of features from tiny images. 2009.

Xiang Li, Chen Shuo, and Yang Jian. Understanding the disharmony between weight normalization family and weight decay. In *AAAI*, 2020.

Zhiyuan Li and Sanjeev Arora. An exponential learning rate schedule for deep learning. In *International Conference on Learning Representations*, 2020. URL https://openreview.net/forum?id=rJg8TeSFDH.

Tsung-Yi Lin, Michael Maire, Serge Belongie, James Hays, Pietro Perona, Deva Ramanan, Piotr Dollár, and C Lawrence Zitnick. Microsoft coco: Common objects in context. In *European conference on computer vision*, pp. 740–755. Springer, 2014.

Tsung-Yi Lin, Piotr Dollár, Ross Girshick, Kaiming He, Bharath Hariharan, and Serge Belongie. Feature pyramid networks for object detection. In *Proceedings of the IEEE conference on computer vision and pattern recognition*, pp. 2117–2125, 2017.

Ping Luo, Xinjiang Wang, Wenqi Shao, and Zhanglin Peng. Towards understanding regularization in batch normalization. In *International Conference on Learning Representations*, 2019. URL https://openreview.net/forum?id=HJlLKjR9FQ.

Ningning Ma, Xiangyu Zhang, Hai-Tao Zheng, and Jian Sun. Shufflenet v2: Practical guidelines for efficient cnn architecture design. In *Proceedings of the European Conference on Computer Vision (ECCV)*, pp. 116–131, 2018.

Chao Peng, Tete Xiao, Zeming Li, Yuning Jiang, Xiangyu Zhang, Kai Jia, Gang Yu, and Jian Sun. Megdet: A large mini-batch object detector. In *Proceedings of the IEEE Conference on Computer Vision and Pattern Recognition*, pp. 6181–6189, 2018.

Boris T Polyak. Some methods of speeding up the convergence of iteration methods. *USSR Computational Mathematics and Mathematical Physics*, 4(5):1–17, 1964.

Olga Russakovsky, Jia Deng, Hao Su, Jonathan Krause, Sanjeev Satheesh, Sean Ma, Zhiheng Huang, Andrej Karpathy, Aditya Khosla, Michael Bernstein, et al. Imagenet large scale visual recognition challenge. *International journal of computer vision*, 115(3):211–252, 2015.

Tim Salimans and Durk P Kingma. Weight normalization: A simple reparameterization to accelerate training of deep neural networks. In *Advances in Neural Information Processing Systems*, pp. 901–909, 2016.

Mark Sandler, Andrew Howard, Menglong Zhu, Andrey Zhmoginov, and Liang-Chieh Chen. Mobilenetv2: Inverted residuals and linear bottlenecks. In *Proceedings of the IEEE conference on computer vision and pattern recognition*, pp. 4510–4520, 2018.

Shibani Santurkar, Dimitris Tsipras, Andrew Ilyas, and Aleksander Madry. How Does Batch Normalization Help Optimization? *arXiv e-prints*, art. arXiv:1805.11604, May 2018.

Wenqi Shao, Tianjian Meng, Jingyu Li, Ruimao Zhang, Yudian Li, Xiaogang Wang, and Ping Luo. Ssn: Learning sparse switchable normalization via sparsestmax. In *Proceedings of the IEEE Conference on Computer Vision and Pattern Recognition*, pp. 443–451, 2019.

Saurabh Singh and Shankar Krishnan. Filter response normalization layer: Eliminating batch dependence in the training of deep neural networks. In *Proceedings of the IEEE/CVF Conference on Computer Vision and Pattern Recognition (CVPR)*, June 2020.

Dmitry Ulyanov, Andrea Vedaldi, and Victor Lempitsky. Instance normalization: The missing ingredient for fast stylization. *arXiv preprint arXiv:1607.08022*, 2016.

Twan van Laarhoven. L2 regularization versus batch and weight normalization. In *Advances in Neural Information Processing Systems*. 2017.

Yuxin Wu and Kaiming He. Group normalization. In *Proceedings of the European Conference on Computer Vision (ECCV)*, pp. 3–19, 2018.

Junjie Yan, Ruosi Wan, Xiangyu Zhang, Wei Zhang, Yichen Wei, and Jian Sun. Towards stabilizing batch statistics in backward propagation of batch normalization. In *International Conference on Learning Representations*, 2020. URL https://openreview.net/forum?id=SkgGjRVKDS.

Guodong Zhang, Chaoqi Wang, Bowen Xu, and Roger Grosse. Three mechanisms of weight decay regularization. In *International Conference on Learning Representations*, 2019. URL https://openreview.net/forum?id=B1lz-3Rct7.

A PROOF OF THEOREMS

Remark 3. *In the following context, we will use the following conclusion multiple times:* $\forall \delta, \varepsilon \in \mathbb{R}$*, if* $|\delta| \ll 1, |\varepsilon| \ll 1$*, then we have:*

$$(1+\delta)^2 \approx 1+2\delta, \quad \sqrt{1+\delta} \approx 1+\frac{\delta}{2}, \quad \frac{1}{1+\delta} \approx 1-\delta, \quad (1+\delta)(1+\varepsilon) \approx 1+\delta+\varepsilon. \tag{23}$$

A.1 PROOF OF LEMMA 1

Proof. Given $\boldsymbol{w}_0 \in \mathbb{R}^p \backslash \{\mathbf{0}\}$, since $\forall k > 0, \mathcal{L}(\boldsymbol{w}_0) = \mathcal{L}(k\boldsymbol{w}_0)$, then we have

$$\frac{\partial \mathcal{L}(\boldsymbol{w})}{\partial \boldsymbol{w}}\Big|_{\boldsymbol{w}=\boldsymbol{w}_0} = \frac{\partial \mathcal{L}(k\boldsymbol{w})}{\partial \boldsymbol{w}}\Big|_{\boldsymbol{w}=\boldsymbol{w}_0} = \frac{\partial \mathcal{L}(\boldsymbol{w})}{\partial \boldsymbol{w}}\Big|_{\boldsymbol{w}=k\boldsymbol{w}_0} \cdot k \tag{24}$$

$$\frac{\partial \mathcal{L}(\boldsymbol{kw})}{\partial k}\Big|_{\boldsymbol{w}=\boldsymbol{w}_0} = \langle \frac{\partial \mathcal{L}(\boldsymbol{w})}{\partial \boldsymbol{w}}\Big|_{\boldsymbol{w}=k\boldsymbol{w}_0}, \boldsymbol{w}_0 \rangle = \frac{1}{k} \cdot \langle \frac{\partial \mathcal{L}(\boldsymbol{w})}{\partial \boldsymbol{w}}\Big|_{\boldsymbol{w}=\boldsymbol{w}_0}, \boldsymbol{w}_0 \rangle = 0 \tag{25}$$

□

A.2 PROOF OF THEOREM 1

Lemma 2. *If the sequence* $\{x_t\}_{t=1}^{\infty}$ *satisfies*

$$x_t \geq \alpha x_{t-1} + \frac{L}{x_{t-1}} \tag{26}$$

. where $x_1 > 0$*,* $L > 0$

Then, we have

$$x_t \geq \sqrt{\frac{L}{1-\alpha}} - \alpha^{t-1} |\sqrt{\frac{L}{1-\alpha}} - x_1| \tag{27}$$

Proof. If $x_t \geq \sqrt{\frac{L}{1-\alpha}}$, since $\sqrt{L/(1-\alpha)} \geq 2\sqrt{\alpha L}$ then we have

$$x_{t+1} \geq \alpha x_t + \frac{L}{x_t} \geq \alpha \sqrt{\frac{L}{1-\alpha}} + \frac{L}{\sqrt{L/(1-\alpha)}} = \sqrt{\frac{L}{1-\alpha}}, \tag{28}$$

which means $\forall k > t, x_k \geq \sqrt{L/(1-\alpha)}$. If $x_t < \sqrt{L/(1-\alpha)}$, then we have

$$\sqrt{\frac{L}{1-\alpha}} - x_{t+1} \leq (\alpha - \frac{\sqrt{L(1-\alpha)}}{x_t})(\sqrt{\frac{L}{1-\alpha}} - x_t) < \alpha(\sqrt{\frac{L}{1-\alpha}} - x_t). \tag{29}$$

Therefore, by deduction we can easily prove if $x_T < \sqrt{L/(1-\alpha)}$, then $\forall t \in [1, T-1]$, we have

$$0 < x_t < x_{t+1} < X_T < \sqrt{\frac{L}{1-\alpha}}, \tag{30}$$

$$(\sqrt{\frac{L}{1-\alpha}} - x_t) < \alpha^{t-1}(\sqrt{\frac{L}{1-\alpha}} - x_1). \tag{31}$$

In summary, we have

$$x_t \geq \sqrt{\frac{L}{1-\alpha}} - \alpha^{t-1} |\sqrt{\frac{L}{1-\alpha}} - x_1| \tag{32}$$

□

Proof of Theorem 1. since $\langle \boldsymbol{w}_t, \boldsymbol{g}_t \rangle = 0$, then we have:

$$||\boldsymbol{w}_{t+1}||_2^2 = (1-\eta\lambda)^2 ||\boldsymbol{w}_t||_2^2 + \frac{||\tilde{\boldsymbol{g}}_t||_2^2 \eta^2}{||\boldsymbol{w}_t||_2^2} \tag{33}$$

Denote x_t as $||\boldsymbol{w}_t||_2^2$, L_t as $||\tilde{\boldsymbol{g}}_t||_2^2$ and omit $O((\eta\lambda)^2)$ part. Then $L_t > l$, $\mathbb{E}[L_t|x_t] = L$, $Var(L_t|x_t) = \mathbb{E}[(L_t - L)^2|x_t] < V$. Eq.(33) is equivalent to

$$x_{t+1} = (1 - 2\lambda\eta)x_t + \frac{L_t\eta^2}{x_t}. \tag{34}$$

According to Lemma 2, we have

$$x_t > \sqrt{\frac{l\eta}{2\lambda}} - (1 - 2\lambda\eta)^{t-1}|x_0 - \sqrt{\frac{l\eta}{2\lambda}}|. \tag{35}$$

Eq.(35) implies when $t > 1 + \frac{log((\sqrt{2}-1)\sqrt{l\eta/(4\lambda)}) - log(|x_0 - \sqrt{l\eta/(4\lambda)}|)}{log(1-2\lambda\eta)}$, we have $x_t > \sqrt{\frac{l\eta}{4\lambda}}$.

Now, denote x^* as the $\sqrt{\frac{L\eta}{2\lambda}}$, then we have

$$\begin{aligned}\mathbb{E}[(x_{t+1} - x^*)^2|x_t] &= \mathbb{E}[((1 - 2\lambda\eta - \frac{L\eta^2}{x_t x^*})(x_t - x^*) + \frac{L_t - L}{x_t})^2|x_t] \\ &= (1 - 2\lambda\eta - \frac{L\eta^2}{x_t x^*})^2(x_t - x^*)^2 + \frac{\mathbb{E}[(L_t - L)^2|x_t]\eta^4}{x_t^2}\end{aligned} \tag{36}$$

If $t > T(\alpha, \lambda, \eta, l, x_0) = 1 + \frac{log((\sqrt{2}-1)\sqrt{l\eta/(4\lambda)}) - log(|x_0 - \sqrt{l\eta/(4\lambda)}|)}{log(1-2\lambda\eta)}$, Eq.(35) implies

$$1 - 2\lambda\eta - \sqrt{\frac{2L}{l}} \cdot 2\lambda\eta < 1 - 2\lambda\eta - \frac{L\eta^2}{x^* x_t}. \tag{37}$$

Combining with assumption 3 in Theorem 1, we can derive $1 - 2\lambda\eta - \sqrt{\frac{2L}{l}} \cdot 2\lambda\eta > 0$, which means

$$0 < 1 - 2\lambda\eta - \frac{L}{x^* x_t}. \tag{38}$$

Combining with Eq.(36), (35), (38), if $t > T(\alpha, \lambda, \eta, l, x_0)$, we have

$$\mathbb{E}[(x_{t+1} - x^*)^2|x_t] < (1 - 2\lambda\eta)^2(x_t - x^*)^2 + \frac{4V\eta^3\lambda}{l}. \tag{39}$$

Considering the expectation with respect to the distribution of x_t, we have

$$\mathbb{E}(x_{t+1} - x^*)^2 < (1 - 2\lambda\eta)^2\mathbb{E}(x_t - x^*)^2 + \frac{4V\eta^3\lambda}{l}. \tag{40}$$

Approximate $(1 - 2\lambda\eta)^2 = 1 - 4\lambda\eta$, and iterate Eq.(40) for $t - T(\alpha, \lambda, \eta, l, x_0)$ times, we have

$$\mathbb{E}(x_t - x^*)^2 < (1 - 4\lambda\eta)^{t - T(\alpha,\lambda,\eta,l,x_0)}\mathbb{E}(x_{T(\alpha,\lambda,\eta,l,x_0)} - x^*)^2 + \frac{V\eta^2}{l}. \tag{41}$$

$T(\alpha, \lambda, \eta, l, x_0)$ is finite, and only depends on $\alpha, \lambda, \eta, l, x_0$. Hence we can set $B = max\{(1 - 4\lambda\eta)^{-t}\mathbb{E}(x_t - x^*)^2 | t = 0, 1, 2, ..., T(\alpha, \lambda, \eta, l, x_0)\}$, note we can prove B is finite by

$$\mathbb{E}x_{t+1}^2 = \mathbb{E}[(1-2\lambda\eta)^2 x_t^2 + 2(1-2\lambda\eta)L_t + \frac{L_t^2}{x_t^2}] < (1-4\lambda\eta)\mathbb{E}x_t^2 + 2(1-2\lambda\eta)L + \frac{V + L^2}{min(x_0^2, l\eta/(2\lambda))}. \tag{42}$$

therefore, $\forall t > 0$, we have

$$\mathbb{E}(x_t - x^*)^2 < (1 - 4\lambda\eta)^t B + \frac{V\eta^2}{l}. \tag{43}$$

□

A.2.1 PROOF OF THEOREM 2

Lemma 3. *Assume $\alpha, \beta, \varepsilon \in (0,1)$, where $\beta << 1$. Denote $diag(1-\frac{2\beta}{1-\alpha}, \alpha, \alpha^2+\frac{2\alpha^2}{1-\alpha}\beta$ as $\mathbf{\Lambda}$, $\boldsymbol{k} = (\frac{1}{(1-\alpha)^2}, -\frac{2\alpha}{(1-\alpha)^2}, \frac{\alpha^2}{(1-\alpha)^2})^T$, $\boldsymbol{e} = (1,1,1)^T$. If $\varepsilon < \frac{1}{3}[\frac{1-\alpha^2}{\beta} - \frac{8}{1-\alpha}]$, then $\forall \boldsymbol{d} \in \mathbb{R}^p$, we have*

$$||(\mathbf{\Lambda} - \varepsilon\beta(1-\alpha)^2\boldsymbol{k}\boldsymbol{e}^T)\boldsymbol{d}||_2^2 < (1-\frac{4\beta}{1-\alpha})||\boldsymbol{d}||_2^2 \tag{44}$$

Proof. Omit $O(\beta^2)$ part, we have

$$||(\mathbf{\Lambda}-\varepsilon\beta(1-\alpha)^2\boldsymbol{k}\boldsymbol{e}^T)\boldsymbol{d}||_2^2 = (1-\frac{4\beta}{1-\alpha})d_1^2+\alpha^2 d_2^2+\alpha^4(1+\frac{4\beta}{1-\alpha})d_3^2-2\varepsilon\beta(d_1+d_2+d_3)(d_1-2\alpha^2 d_2+\alpha^4 d_3) \tag{45}$$

$$\begin{aligned}
&(d_1+d_2+d_3)(d_1-2\alpha^2 d_2+\alpha^4 d_3)\\
=&\frac{[d_1+(1-2\alpha^2)d_2]^2}{2}+\frac{[d_1+(1+\alpha^4)d_3]^2}{2}-(1/2+2\alpha^4)d_2^2-\frac{1+\alpha^8}{2}+(\alpha^4-2\alpha^2)d_2d_3\\
\geq&-(\frac{1}{2}+2\alpha^4+\frac{\alpha^4}{2})d_2^2-(\frac{\alpha^8}{2}+\frac{\alpha^4}{2}-2\alpha^2+\frac{5}{2})d_3^2\\
\geq&-3d_2^2-\frac{5}{2}d_3^2.
\end{aligned} \tag{46}$$

Then we have

$$||(\mathbf{\Lambda} - \varepsilon\beta(1-\alpha)^2\boldsymbol{k}\boldsymbol{e}^T)\boldsymbol{d}||_2^2 \leq (1-\frac{4\beta}{1-\alpha})d_1^2+(\alpha^2+3\beta\varepsilon)d_2^2+(\alpha^4+\frac{4\beta\alpha^4}{1-\alpha}+\frac{5\beta\varepsilon}{2})d_3^2. \tag{47}$$

Since $\varepsilon < \frac{1}{3}[\frac{1-\alpha^2}{\beta} - \frac{8}{1-\alpha}]$, we can prove

$$\alpha^2+3\beta\varepsilon < 1-\frac{4\beta}{1-\alpha}, \tag{48}$$

$$\alpha^4+\frac{4\beta\alpha^4}{1-\alpha}+\frac{5\beta\varepsilon}{2} < 1-\frac{4\beta}{1-\alpha}. \tag{49}$$

Hence, we have

$$||(\mathbf{\Lambda} - \varepsilon\beta(1-\alpha)^2\boldsymbol{k}\boldsymbol{e}^T)\boldsymbol{d}||_2^2 < (1-\frac{4\beta}{1-\alpha})||\boldsymbol{d}||_2^2 \tag{50}$$

□

Proof of Theorem 2. The update rule is

$$\begin{aligned}
\boldsymbol{w}_{t+1} &= \boldsymbol{w}_t - \eta\boldsymbol{v}_t\\
&= \boldsymbol{w}_t - \eta(\alpha\boldsymbol{v}_{t-1}+\frac{\tilde{\boldsymbol{g}}_t}{||\boldsymbol{w}_t||}+\lambda\boldsymbol{w}_t)\\
&= \boldsymbol{w}_t - \eta(\alpha\frac{\boldsymbol{w}_{t-1}-\boldsymbol{w}_t}{\eta}+\frac{\tilde{\boldsymbol{g}}_t}{||\boldsymbol{w}_t||}+\lambda\boldsymbol{w}_t)\\
&= (1-\eta\lambda+\alpha)\boldsymbol{w}_t-\alpha\boldsymbol{w}_{t-1}-\boldsymbol{g}_t\eta.
\end{aligned} \tag{51}$$

Then we have

$$\begin{aligned}
||\boldsymbol{w}_{t+1}||_2^2 &= (1-\eta\lambda+\alpha)^2||\boldsymbol{w}_t||_2^2-2\alpha(1+\alpha-\eta\lambda)\langle\boldsymbol{w}_t,\boldsymbol{w}_{t-1}\rangle+\alpha^2||\boldsymbol{w}_{t-1}||_2^2\\
&+||\boldsymbol{g}_t||_2^2\eta^2+2\langle\alpha\boldsymbol{w}_{t-1},\boldsymbol{g}_t\eta\rangle\\
&= (1-\eta\lambda+\alpha)^2||\boldsymbol{w}_t||_2^2-2\alpha(1+\alpha-\eta\lambda)\langle\boldsymbol{w}_t,\boldsymbol{w}_{t-1}\rangle+\alpha^2||\boldsymbol{w}_{t-1}||_2^2\\
&+||\boldsymbol{g}_t||_2^2\eta^2+2\langle\alpha(\boldsymbol{w}_t+\eta\boldsymbol{v}_{t-1}),\boldsymbol{g}_t\eta\rangle\\
&= (1-\eta\lambda+\alpha)^2||\boldsymbol{w}_t||_2^2-2\alpha(1+\alpha-\eta\lambda)\langle\boldsymbol{w}_t,\boldsymbol{w}_{t-1}\rangle+\alpha^2||\boldsymbol{w}_{t-1}||_2^2\\
&+\frac{\tilde{h}_t\eta^2}{||\boldsymbol{w}_t||_2^2}.
\end{aligned} \tag{52}$$

$$\langle \boldsymbol{w}_{t+1}, \boldsymbol{w}_t \rangle = (1+\alpha-\lambda\eta)||\boldsymbol{w}_t||^2 - \alpha\langle \boldsymbol{w}_t, \boldsymbol{w}_{t-1}\rangle, \tag{53}$$

Let $\boldsymbol{X}_t, \boldsymbol{A}, \boldsymbol{e}$ denote:

$$\boldsymbol{X}_t = \begin{pmatrix} ||\boldsymbol{w}_t||_2^2 \\ \langle \boldsymbol{w}_t, \boldsymbol{w}_{t-1}\rangle \\ ||\boldsymbol{w}_{t-1}||_2^2 \end{pmatrix}, \tag{54}$$

$$\boldsymbol{A} = \begin{pmatrix} (1+\alpha-\lambda\eta)^2 & -2\alpha(1+\alpha-\lambda\eta) & \alpha^2 \\ 1+\alpha-\lambda\eta & -\alpha & 0 \\ 1 & 0 & 0 \end{pmatrix}, \tag{55}$$

$$\boldsymbol{e} = \begin{pmatrix} 1 \\ 0 \\ 0 \end{pmatrix}, \tag{56}$$

$$\tag{57}$$

respectively. The Eq.(52), (53) can be formulated as

$$\boldsymbol{X}_{t+1} = \boldsymbol{A}\boldsymbol{X}_t + \frac{\tilde{h}_t\eta^2}{\boldsymbol{e}^T\boldsymbol{X}_t}\boldsymbol{e}. \tag{58}$$

When $\lambda\eta < (1-\sqrt{\alpha})^2$, the eigen value of $\boldsymbol{A}$ are all real number:

$$\lambda_1 = \frac{(1+\alpha-\lambda\eta)^2 + (1+\alpha-\lambda\eta)\sqrt{(1+\alpha-\lambda\eta)^2-4\alpha}}{2} - \alpha = 1 - \frac{2\lambda\eta}{1-\alpha} + O(\lambda^2\eta^2), \tag{59}$$

$$\lambda_2 = \alpha, \tag{60}$$

$$\lambda_3 = \frac{(1+\alpha-\lambda\eta)^2 - (1+\alpha-\lambda\eta)\sqrt{(1+\alpha-\lambda\eta)^2-4\alpha}}{2} - \alpha = \alpha^2 + \frac{2\alpha^2}{(1-\alpha)}\lambda\eta + O(\lambda^2\eta^2), \tag{61}$$

and it's easy to prove

$$0 < \lambda_3 < \lambda_2 = \alpha < \lambda_1 < 1. \tag{62}$$

Therefore, $\boldsymbol{A}$ can be formulated as

$$\boldsymbol{S}^{-1}\boldsymbol{A}\boldsymbol{S} = \boldsymbol{\Lambda}, \tag{63}$$

where $\boldsymbol{\Lambda}$ is a diagonal matrix whose diagonal elements are the eigen value of $\boldsymbol{A}$; the column vector of $\boldsymbol{S}$ is the eigen vectors of $\boldsymbol{A}$, note the fromulation of $\boldsymbol{S}, \boldsymbol{\Lambda}$ are not unique. Specifically, we set $\boldsymbol{\Lambda}, \boldsymbol{S}$ as

$$\boldsymbol{\Lambda} = \begin{pmatrix} \lambda_1 & 0 & 0 \\ 0 & \lambda_2 & 0 \\ 0 & 0 & \lambda_3 \end{pmatrix}, \tag{64}$$

$$\boldsymbol{S} = \begin{pmatrix} 1 & 1 & 1 \\ \frac{1+\alpha-\lambda\eta}{\alpha+\lambda_1} & \frac{1+\alpha-\lambda\eta}{\alpha+\lambda_2} & \frac{1+\alpha-\lambda\eta}{\alpha+\lambda_3} \\ \frac{1}{\lambda_1} & \frac{1}{\lambda_2} & \frac{1}{\lambda_3} \end{pmatrix}. \tag{65}$$

Moreover, the inverse of $\boldsymbol{S}$ exists, and can be explicitly expressed as

$$\boldsymbol{S}^{-1} = \begin{pmatrix} \frac{(\alpha+\lambda_1)\lambda_1}{(\lambda_1-\alpha)(\lambda_1-\lambda_3)} & -\frac{2\lambda_1(\alpha+\lambda_1)(\alpha+\lambda_3)}{(\lambda_1-\lambda_3)(\lambda_1-\alpha)(1+\alpha-\beta)} & \frac{\lambda_1\lambda_3(\alpha+\lambda_1)}{(\lambda_1-\alpha)(\lambda_1-\lambda_3)} \\ -\frac{2\alpha^2}{(\lambda_1-\alpha)(\alpha-\lambda_3)} & \frac{2\alpha(\alpha+\lambda_1)(\alpha+\lambda_3)}{(\lambda_1-\alpha)(\alpha-\lambda_3)(1+\alpha-\beta)} & -\frac{2\alpha\lambda_1\lambda_3}{(\lambda_1-\alpha)(\alpha-\lambda_3)} \\ \frac{(\alpha+\lambda_3)\lambda_3}{(\alpha-\lambda_3)(\lambda_1-\lambda_3)} & -\frac{2\lambda_3(\alpha+\lambda_3)(\alpha+\lambda_1)}{(\lambda_1-\lambda_3)(\alpha-\lambda_3)(1+\alpha-\beta)} & \frac{(\alpha+\lambda_3)\lambda_1\lambda_3}{(\alpha-\lambda_3)(\lambda_1-\lambda_3)} \end{pmatrix}. \tag{66}$$

let $\boldsymbol{Y}_t = \boldsymbol{S}^{-1}\boldsymbol{X}_t$, combining with Eq.(58), we have

$$\boldsymbol{Y}_{t+1} = \boldsymbol{\Lambda}\boldsymbol{Y}_t + \frac{\tilde{h}_t\eta^2}{(\boldsymbol{S}^T\boldsymbol{e})^T\boldsymbol{Y}_t}\boldsymbol{S}^{-1}\boldsymbol{e}. \tag{67}$$

Combining with Eq.(65) and Eq.(66), and set $\boldsymbol{Y}_t = (\tilde{a}_t, \tilde{b}_t, \tilde{c}_t)^T$, we can rewritten Eq.(67) as

$$\begin{aligned}
\tilde{a}_{t+1} &= \lambda_1 \tilde{a}_t + \frac{\tilde{h}_t \eta^2}{\tilde{a}_t + \tilde{b}_t + \tilde{c}_t} \cdot \frac{(\alpha + \lambda_1)\lambda_1}{(\lambda_1 - \alpha)(\lambda_1 - \lambda_3)}, && (68)\\
\tilde{b}_{t+1} &= \alpha \tilde{b}_t - \frac{\tilde{h}_t \eta^2}{\tilde{a}_t + \tilde{b}_t + \tilde{c}_t} \cdot \frac{2\alpha^2}{(\lambda_1 - \alpha)(\alpha - \lambda_3)}, && (69)\\
\tilde{c}_{t+1} &= \lambda_3 \tilde{c}_t + \frac{\tilde{h}_t \eta^2}{\tilde{a}_t + \tilde{b}_t + \tilde{c}_t} \cdot \frac{(\alpha + \lambda_3)\lambda_3}{(\alpha - \lambda_3)(\lambda_1 - \lambda_3)}. && (70)
\end{aligned}$$

Note $||\boldsymbol{w}_t||_2^2 = \tilde{a}_t + \tilde{b}_t + \tilde{c}_t$. Now we can prove the following inequations by mathematical induction

$$\begin{aligned}
\tilde{b}_t &< 0, && (71)\\
\tilde{c}_t &> 0, && (72)\\
(\alpha - \lambda_1)\tilde{b}_t &> (\lambda_1 - \lambda_3)\tilde{c}_t, && (73)\\
\tilde{a}_t + \tilde{b}_t + \tilde{c}_t &> 0, && (74)\\
\tilde{a}_{t+1} + \tilde{b}_{t+1} + \tilde{c}_{t+1}, &> \lambda_1(\tilde{a}_t + \tilde{b}_t + \tilde{c}_t) + \frac{\tilde{h}_t \eta^2}{\tilde{a}_t + \tilde{b}_t + \tilde{c}_t}, && (75)
\end{aligned}$$

Since the start point $\boldsymbol{X}_1 = (a_1, a_1, a_1)^T$ ($a_1 > 0$), the start point $\boldsymbol{Y}_1 = \boldsymbol{S}^{-1}\boldsymbol{X}_1$. Combining with Eq.(66), we have

$$\begin{aligned}
\tilde{b}_1 &= -\frac{2\alpha^2 \lambda \eta}{(\lambda_1 - \alpha)(\alpha - \lambda_3)} a_1, && (76)\\
\tilde{c}_1 &= \frac{\lambda_3(\lambda_3 + \alpha)(1 - \alpha + \lambda\eta)}{(\lambda_3 - \alpha)(\lambda_1 - \lambda_3)(1 + \alpha - \lambda\eta)} \left(\frac{1 - \alpha - \lambda\eta}{1 - \alpha + \lambda\eta} - \lambda_1\right) a_1, && (77)
\end{aligned}$$

by which it's easy to prove $(\alpha - \lambda_1)\tilde{b}_1 > (\lambda_1 - \lambda_3)\tilde{c}_1$. Besides $\tilde{a}_1 + \tilde{b}_1 + \tilde{c}_1 = \boldsymbol{e}^T \boldsymbol{S} \boldsymbol{Y}_1 = \boldsymbol{e}^T \boldsymbol{X}_1 = a_1 > 0$.

Suppose for $t = T$, Eq. (71), (72), (73), (74) hold, combining with Eq.(69), (70), we can derive $\tilde{b}_{T+1} < 0, \tilde{a}_{T+1} > 0$, so Eq.(71), (72) hold for $t = T + 1$; Besides, we have

$$\begin{aligned}
(\alpha - \lambda_1)\tilde{b}_{T+1} &= \alpha(\alpha - \lambda_1)\tilde{b}_T + \frac{\tilde{h}_t \eta^2}{\tilde{a}_T + \tilde{b}_T + \tilde{c}_T} \cdot \frac{2\alpha^2}{(\alpha - \lambda_3)}\\
&> \lambda_3(\lambda_1 - \lambda_3)\tilde{c}_T + \frac{\tilde{h}_t \eta^2}{\tilde{a}_T + \tilde{b}_T + \tilde{c}_T} \cdot \frac{(\alpha + \lambda_3)\lambda_3}{(\alpha - \lambda_3)}\\
&= (\lambda_1 - \lambda_3)\tilde{c}_{T+1}, && (78)
\end{aligned}$$

thus Eq.(73) holds for $t = T + 1$. Sum Eq.(68), Eq.(69), Eq.(70), due to Eq.(73) we have

$$\begin{aligned}
\tilde{a}_{T+1} + \tilde{b}_{T+1} + \tilde{c}_{T+1} &= \lambda_1 \tilde{a}_T + \alpha \tilde{b}_T + \lambda_3 \tilde{c}_T + \frac{\tilde{h}_t \eta^2}{\tilde{a}_T + \tilde{b}_T + \tilde{c}_T}\\
&> \lambda_1(\tilde{a}_T + \tilde{b}_T + \tilde{c}_T) + \frac{\tilde{h}_t \eta^2}{\tilde{a}_T + \tilde{b}_T + \tilde{c}_T}, && (79)
\end{aligned}$$

Eq.(75) holds for $t = T + 1$, combining with the fact that $\tilde{a}_T + \tilde{b}_T + \tilde{c}_T > 0$, we have $\tilde{a}_{T+1} + \tilde{b}_{T+1} + \tilde{c}_{T+1} > 0$.

According to Lemma 2, we can estimate the lower bound of $\tilde{a}_t + \tilde{b}_t + \tilde{c}_t$: when $t > 1 + \frac{log((\sqrt{2}-1)\sqrt{l\eta/(4\lambda)}) - log(|||\boldsymbol{w}_0||_2^2 - \sqrt{l\eta/(4\lambda)}|)}{log(1-2\lambda\eta)}$,

$$\tilde{a}_t + \tilde{b}_t + \tilde{c}_t \geq \sqrt{\frac{l\eta}{2(1-\lambda_1)}} \approx \sqrt{\frac{l\eta(1-\alpha)}{4\lambda}} \qquad (80)$$

Now we can analyze the expectation of distance(l^2 norm) between $\boldsymbol{Y}_t = (\tilde{a}_t, \tilde{b}_t, \tilde{c}_t)^T$ and the fixed point $\boldsymbol{Y}^* = (\tilde{a}^*, \tilde{b}^*, \tilde{c}^*)^T$ which satisfies

$$\boldsymbol{Y}^* = \boldsymbol{\Lambda}\boldsymbol{Y}^* + \frac{L\eta^2}{(\boldsymbol{S}^T\boldsymbol{e})^T\boldsymbol{Y}^*}\boldsymbol{S}^{-1}\boldsymbol{e}. \tag{81}$$

Assume $x_t = \tilde{a}_t + \tilde{b}_t + \tilde{c}_t$, $x^* = \tilde{a}^* + \tilde{b}^* + \tilde{c}^* > 0$, then we have:

$$\boldsymbol{Y}_{t+1} - \boldsymbol{Y}^* = (\boldsymbol{\Lambda} - \frac{L\eta^2}{x_t x^*}\boldsymbol{k}\boldsymbol{e}^T)(\boldsymbol{Y}_t - \boldsymbol{Y}^*) + \frac{(\tilde{h}_t - L)\eta^2}{x_t}\boldsymbol{k} \tag{82}$$

where $\boldsymbol{k} = (k_1, k_2, k_3)^T = \boldsymbol{S}^{-1}\boldsymbol{e}$. In the following context, will omit the $O(\lambda^2\eta^2)$ part since $\lambda\eta \ll 1$. k_1, k_2, k_3 can be approximated as

$$k_1 = \frac{1}{(1-\alpha)^2} + O(\beta), \tag{83}$$

$$k_2 = -\frac{2\alpha}{(1-\alpha)^2} + O(\beta), \tag{84}$$

$$k_3 = \frac{\alpha^2}{(1-\alpha)^2} + O(\beta). \tag{85}$$

Then we have

$$\mathbb{E}[||\boldsymbol{Y}_{t+1} - \boldsymbol{Y}^*||_2^2|\boldsymbol{Y_t}] = ||(\boldsymbol{\Lambda} - \frac{L}{x_t x^*}\boldsymbol{k}\boldsymbol{e}^T)(\boldsymbol{Y}_t - \boldsymbol{Y}^*)||_2^2 + \frac{\mathbb{E}[(\tilde{h}_t - L)^2|\boldsymbol{Y_t}]\eta^4}{x_t^2}||\boldsymbol{k}||_2^2 \tag{86}$$

It's easy to obtain the value of fixed point $x^* = \tilde{a}^* + \tilde{b}^* + \tilde{c}^* = \sqrt{\frac{L\eta}{\lambda(1-\alpha)(2-\frac{\lambda\eta}{1+\alpha})}}$, and we have known that if $t > 1 + \frac{log((\sqrt{2}-1)\sqrt{l\eta/(4\lambda)}) - log(|||\boldsymbol{w}_0||_2^2 - \sqrt{l\eta/(4\lambda)}|)}{log(1-2\lambda\eta)}$, $x_t > \sqrt{\frac{l\eta(1-\alpha)}{4\lambda}}$,, therefore we have

$$\frac{L\eta^2}{x_t x^*} < \sqrt{\frac{2L}{l}} \cdot 2\lambda\eta, \tag{87}$$

$$\frac{\mathbb{E}[(\tilde{h}_t - L)^2|\boldsymbol{Y_t}]}{x_t^2}\eta^4 < \frac{4V\eta^3\lambda}{l(1-\alpha)}. \tag{88}$$

According to assumption 3, we can prove

$$\sqrt{\frac{2L}{l}} < \frac{(1-\alpha)^2}{3}[\frac{1-\alpha^2}{\beta} - \frac{8}{1-\alpha}], \tag{89}$$

combining with Lemma 3, we have

$$\mathbb{E}[||\boldsymbol{Y}_{t+1} - \boldsymbol{Y}^*||_2^2|\boldsymbol{Y_t}] < (1 - \frac{4\lambda\eta}{1-\alpha})||\boldsymbol{Y}_t - \boldsymbol{Y}^*||_2^2 + \frac{4V\eta^3\lambda||\boldsymbol{k}||_2^2}{l(1-\alpha)}, \tag{90}$$

which implies

$$\mathbb{E}||\boldsymbol{Y}_{t+1} - \boldsymbol{Y}^*||_2^2 < (1 - \frac{4\lambda\eta}{1-\alpha})^{t-T}\mathbb{E}||\boldsymbol{Y}_T - \boldsymbol{Y}^*||_2^2 + \frac{V\eta^2(1+4\alpha^2+\alpha^4)}{l(1-\alpha)^4}, \tag{91}$$

where $T = [1 + \frac{log((\sqrt{2}-1)\sqrt{l\eta/(4\lambda)}) - log(|||\boldsymbol{w}_0||_2^2 - \sqrt{l\eta/(4\lambda)}|)}{log(1-2\lambda\eta)}]$. Therefore, similar to the proof of theorem 1, $\exists B > 0$,

$$\mathbb{E}||\boldsymbol{Y}_{t+1} - \boldsymbol{Y}^*||_2^2 < (1 - \frac{4\lambda\eta}{1-\alpha})^t B + \frac{V\eta^2(1+4\alpha^2+\alpha^4)}{l(1-\alpha)^4}. \tag{92}$$

Recall $||\boldsymbol{w}_t||_2^2 = \boldsymbol{e}^T\boldsymbol{Y}_t$, therefore

$$\mathbb{E}[||\boldsymbol{w}_t||_2^2 - (w^*)^2]^2 \leq 3\mathbb{E}||\boldsymbol{Y}_{t+1} - \boldsymbol{Y}^*||_2^2 < 3(1 - \frac{4\lambda\eta}{1-\alpha})^t B + \frac{3V\eta^2(1+4\alpha^2+\alpha^4)}{l(1-\alpha)^4}. \tag{93}$$

□

Remark 4. *By Eq.(93), the variance of $||\boldsymbol{w}_t||_2^2$ is bounded by $\frac{3V\eta^2(1+4\alpha^2+\alpha^4)}{l(1-\alpha)^4}$, which is not small enough. But we somehow can reduce it: according to Eq.(88), if x_t is close to its theoretical value, then $\frac{\mathbb{E}[(\tilde{h}_t - L)^2|\boldsymbol{Y_t}]}{x_t^2}\eta^4 < \frac{4V\eta^3\lambda(1-\alpha)}{l}$, hence variance of $||\boldsymbol{w}_t||_2^2$ can be bounded by $\frac{3V\eta^2(1+4\alpha^2+\alpha^4)}{2L(1-\alpha)^2}$.*

A.3 PROOF OF THEOREM 3

Proof. In SGD case, we have

$$\langle \boldsymbol{w}_{t+1}, \boldsymbol{w}_t \rangle = (1-\lambda\eta)||\boldsymbol{w}_t||_2^2, \tag{94}$$

then we have

$$cos^2\Delta_t = \frac{\langle \boldsymbol{w}_{t+1}, \boldsymbol{w}_t \rangle^2}{||\boldsymbol{w}_t||_2^2 \cdot ||\boldsymbol{w}_{t+1}||_2^2} = (1-2\lambda\eta)\frac{||\boldsymbol{w}_t||_2^2}{||\boldsymbol{w}_{t+1}||_2^2}. \tag{95}$$

Accoring to Theorem 1, when $V=0$, we have

$$|\frac{||\boldsymbol{w}_t||_2^2}{(w^*)^2} - 1| < O((1-2\lambda\eta)^T), \tag{96}$$

which implies

$$|\Delta_t^2 - 2\lambda\eta| = |cos^2\Delta_t - 1 + 2\lambda\eta| < O((1-2\lambda\eta)^T). \tag{97}$$

Since Δ_t and $\sqrt{2\lambda\eta}$ are both finite, we have

$$|\Delta_t - \sqrt{2\lambda\eta}| < O((1-2\lambda\eta)^T). \tag{98}$$

In SGDM case, according to theorem 2, when $V=0$, Eq.(92 implies

$$|||\boldsymbol{w}_t||_2^2 - (w^*)^2| \quad < \quad O((1-\frac{2\lambda\eta}{1-\alpha})^t), \tag{99}$$

$$|\langle \boldsymbol{w}_{t+1}, \boldsymbol{w}_t \rangle^2 - \frac{1+\alpha-2\lambda\eta}{1+\alpha}(w^*)^2| \quad < \quad O((1-\frac{2\lambda\eta}{1-\alpha})^t). \tag{100}$$

Therefore it is easy to derive

$$|\Delta_t^2 - \frac{2\lambda\eta}{1+\alpha}| = |cos^2\Delta_t - 1 + \frac{2\lambda\eta}{1+\alpha}| < O((1-\frac{2\lambda\eta}{1+\alpha})^T). \tag{101}$$

Since Δ_t and $\sqrt{\frac{2\lambda\eta}{1+\alpha}}$ are both finite, we have

$$|\Delta_t - \sqrt{\frac{2\lambda\eta}{1+\alpha}}| < O((1-\frac{2\lambda\eta}{1+\alpha})^T). \tag{102}$$

□

A.4 PROOF OF COROLLARY 3.1

Proof of Corollary 3.1. In SGD case, and Eq.(34), we have

$$||\boldsymbol{w}_{t+1}||_2^2 > (1-2\lambda\eta)||\boldsymbol{w}_t||_2^2, \tag{103}$$

which means

$$||\boldsymbol{w}_{t+T}||_2^2 > (1-2\lambda\eta)^T||\boldsymbol{w}_t||_2^2. \tag{104}$$

On the other hand, we know that when η is divided by k, $||\boldsymbol{w}_t||_2^2$ should be divided by $\sqrt{k}$ to reach the new equilibrium condition, therefore we have

$$\frac{||\boldsymbol{w}_{t+T}||^2}{||\boldsymbol{w}_t||^2} = \frac{1}{\sqrt{k}} > (1-2\lambda\eta)^T. \tag{105}$$

Since $\lambda\eta \ll 1$, $\log(1-2\lambda\eta) \approx -2\lambda\eta$, thus

$$T > \frac{\log(k)}{4\lambda\eta}. \tag{106}$$

.

In SGDM case, by Eq.(79), we have

$$||\boldsymbol{w}_{t+1}||_2^2 > (1-\frac{2\lambda\eta}{1-\alpha})||\boldsymbol{w}_t||_2^2, \tag{107}$$

Similar to SGD case, we have

$$T > \frac{\log(k)(1-\alpha)}{4\lambda\eta}. \tag{108}$$

. □

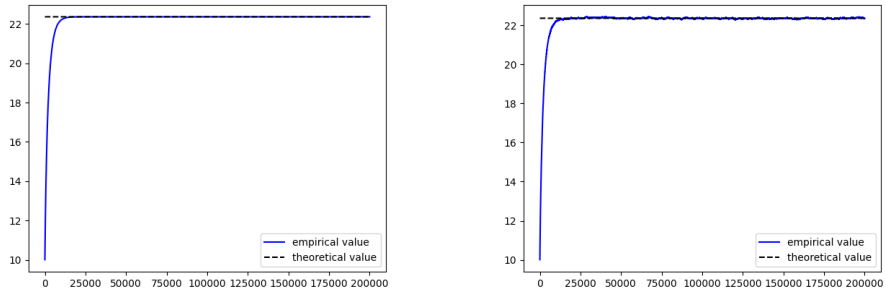
B EXPERIMENTS

B.1 EXPERIMENTS ON SYTHETIC DATA

In this section we apply experiments on sythetic data to prove our claim in section 4: theorem 1 only requires expected square norm of unit gradient is locally steady, it do not need to remain unchanged across the whole training. The proof of theorem implies square norm of weight is determined by the following iterative map:

$$x_{t+1} = (1 - 2\lambda\eta)x_t + \frac{L_t\eta^2}{x_t}, \tag{109}$$

where $\lambda, \eta \in (0, 1)$, L_t denotes the square of unit gradient norm. Hence we simulate x_t with different type of $\{L_t\}_{t=1}^{\infty}$. Results in Figure 4 shows as long as the local variance of square norm of unit gradient is not too much, and expectation of L_t changes smoothly, weight norm can quickly converge to its theoretical value base on expectation of square norm of unit gradient.



(a) $L_t = 10$ (b) $L_t = 10 + \epsilon_t$

(c) $L_t = 10 + sin(\frac{t}{10^5})$ (d) $L_t = 10 + sin(\frac{t}{10^5}) + \epsilon_t$

Figure 4: Simulation of Eq.(109), $\eta = 0.1$, $\lambda = 0.001$, $x_0 = 10$, $\epsilon_t \sim \mathcal{U}(-3, 3)$.

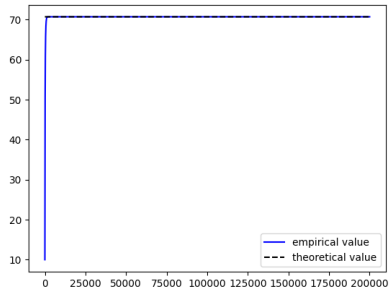
We also simulate SGDM case by following iteration map

$$\boldsymbol{X}_{t+1} = \boldsymbol{A}\boldsymbol{X}_t + \frac{L_t\eta^2}{\boldsymbol{X}_t[0]} \cdot \boldsymbol{e}, \tag{110}$$

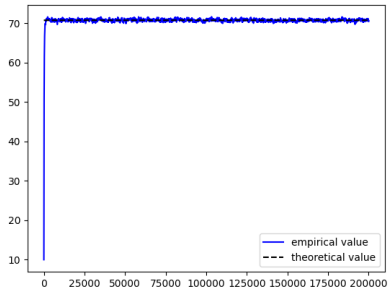
where $\boldsymbol{A}$, $\boldsymbol{X}_t$, $\boldsymbol{e}$ is defined as Eq.(54), (55), (56). Simulation results is shown in Figure 5.

B.2 RETHINKING LINEAR SCALING PRINCIPLE IN SPHERICAL MOTION DYNAMICS

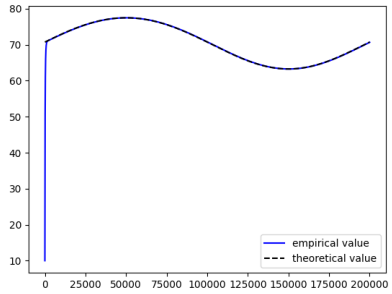
In this section, we will discuss the effect of Linear Scaling Principle (LSP) under the view of SMD. Linear Scaling Principle is proposed by Goyal et al. (2017) to tune the learning rate η with batch size B by $\eta \propto B$. The intuition of LSP is if weights do not change too much within k iterations,



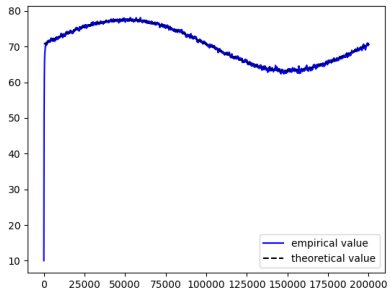
(a) $L_t = 10$



(b) $L_t = 10 + \epsilon_t$



(c) $L_t = 10 + sin(\frac{t}{10^5})$



(d) $L_t = 10 + sin(\frac{t}{10^5}) + \epsilon_t$

Figure 5: Simulation of Eq.(109), $\eta = 0.1$, $\lambda = 0.001$, $x_0 = 10$, $\epsilon_t \sim \mathcal{U}(-3, 3)$, $\alpha = 0.9$.

then k iterations of SGD with learning rate η and minibatch size B (Eq.(111)) can be approximated by a single iteration of SGD with learning rate $k\eta$ and minibatch size kB (Eq.(112):

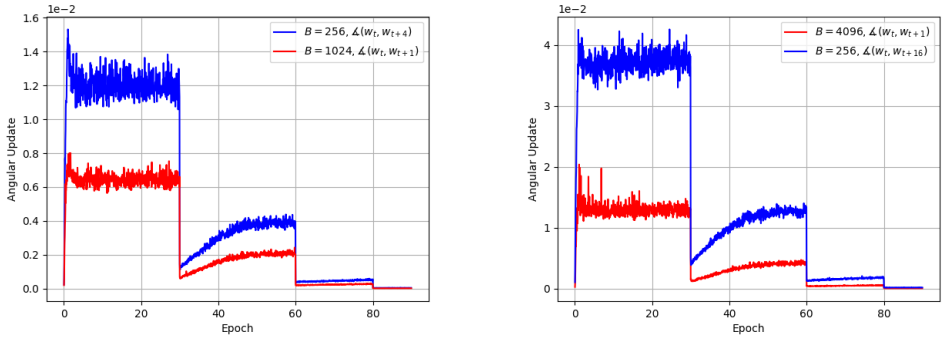
$$\boldsymbol{w}_{t+k} = \boldsymbol{w}_t - \eta \sum_{j<k} (\frac{1}{B} \sum_{x \in \mathcal{B}_j} \frac{\partial \boldsymbol{L}}{\partial \boldsymbol{w}}\Big|_{\boldsymbol{w}_{t+j}, x} + \lambda \boldsymbol{w}_{t+j}), \tag{111}$$

$$\boldsymbol{w}_{t+1} = \boldsymbol{w}_t - k\eta (\frac{1}{kB} \sum_{j<k} \sum_{x \in \mathcal{B}_j} \frac{\partial \boldsymbol{L}}{\partial \boldsymbol{w}}\Big|_{\boldsymbol{w}_t, x} + \lambda \boldsymbol{w}_t). \tag{112}$$

Goyal et al. (2017) shows that combining with gradual warmup, LSP can enlarge the batch size up to $8192(256 \times 32)$ without severe degradation on ImageNet experiments.

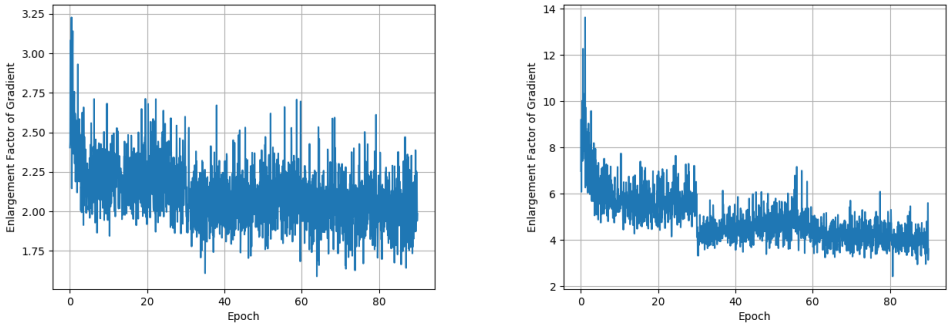
LSP has been proven extremely effective in a wide range of applications. However, from the perspective of SMD, the angular update mostly relies on the pre-defined hyper-parameters, and it is hardly affected by batch size. To clarify the connection between LSP and SMD, we explore the learning dynamics of DNN with different batch size by conducting extensive experiments with ResNet50 on ImageNet, the training settings rigorously follow Goyal et al. (2017): momentum coefficient is $\alpha = 10^{-4}$; WD coefficient is $\lambda = 10^{-4}$; Batch size is denoted by B; learning rate is initialized as $\frac{B}{256} \cdot 0.1$; Total training epoch is 90 epoch, and learning rate is divided by 10 at 30, 60, 80 epoch respectively.

The results of experiments(Figure 6, 7) suggests that the assumption of LSP does not always hold in practice because of three reasons: first, the approximate equivalence between a single iteration in large batch setting, and multiple iterations in small batch setting can only hold in pure SGD formulation, but momentum method is far more commonly used; Second, according Theorem 2, the enlargement ratio of angular update is only determined by the increase factor of learning rate. Figure 6 shows in practice, the accumulated angular update $\measuredangle(\boldsymbol{w}_t, \boldsymbol{w}_{t+k})$ in small batch batch setting is much larger than angular update $\measuredangle(\boldsymbol{w}_t, \boldsymbol{w}_{t+1})$ of a single iteration in larger batch setting when using Linear Scaling Principle; Third, even in pure SGD cases, the enlargement of angular update



(a) $B = 256$ versus $B = 1024$ (b) $B = 256$ versus $B = 4096$

Figure 6: Angular update of weights from layer1.0.conv2 in ResNet50. The blue lines represent the angular update of weights within a single iteration in when batch settings is $B = 1024(4096)$; The red lines represent the accumulated angular update within 4(16) iterations in smaller batch setting($B = 256$).



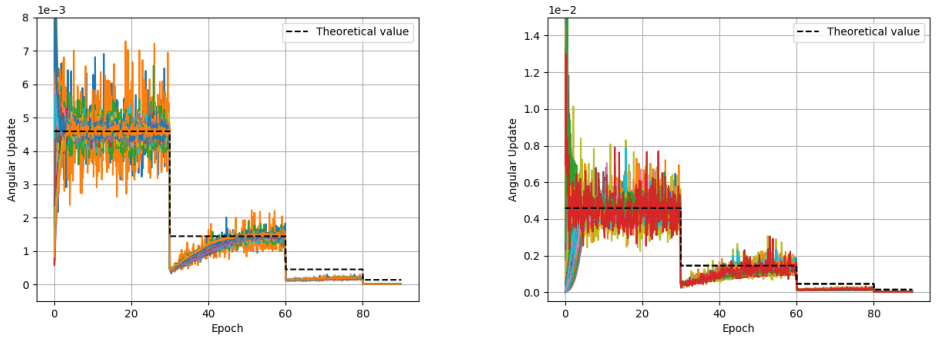
(a) $\frac{||\boldsymbol{g}^{(1024)}||}{||\boldsymbol{g}^{(256)}||}$ (b) $\frac{||\boldsymbol{g}^{(4096)}||}{||\boldsymbol{g}^{(256)}||}$

Figure 7: Enlargement ratio of gradients' norm of weights from layer1.0.conv2 when batch size increases . $||\boldsymbol{g}^{(k)}||$ represents the gradient's norm computed using k samples(not average).

still relies on the increase of learning rate, and has no obvious connection to the enlargement of gradient's norm when equilibrium condition is reached (see Figure 7).

In conclusion, though LSP usually works well in practical applications, SMD suggests we can find more sophisticated and reasonable schemes to tune the learning rate when batch size increases.

B.3 Spherical Motion Dynamics with Different Network Structures



(a) Angle Update of MobileNet-V2 (b) Angular Update of ShuffleNet-V2+

Figure 8: The angular update $\mathbf{\Delta}_t$ of MobileNet-V2Sandler et al. (2018) and ShuffleNet-V2+Ma et al. (2018). The solid lines with different colors represent all scale-invariant weights from the model; The dash black line represents the theoretical value of angular update, which is computed by $\sqrt{\frac{2\lambda\eta}{1+\alpha}}$. Learning rate η is initialized as 0.5, and divided by 10 at epoch 30, 60, 80 respectively; WD coefficient λ is 4×10^{-5}; Momentum parameter α is set as 0.9.